Supporting Information

Hyperconjugation promoted by hydrogen bondings between His98/His241 and carboxyl group contributes to tyrosine decarboxylase catalysis

Jie Ni[1], Guochao Xu[1], Wei Dai[1], Yilei Zhao[2,*] and Ye Ni[1,*]

[1] *Key Laboratory of Industrial Biotechnology, Ministry of Education, School of Biotechnology, Jiangnan University, Wuxi 214122, Jiangsu, China*

[2] *State Key Laboratory of Microbial Metabolism, Joint International Research Laboratory of Metabolic and Developmental Sciences, MOE-LSB and MOE-LSC, School of Life Sciences and Biotechnology, Shanghai Jiao Tong University, Shanghai 200240, China*

*Corresponding authors: yni@jiangnan.edu.cn (Y Ni); yileizhao@sjtu.edu.cn (Y Zhao).

Materials and methods

1.1 Materials

Reagents—L-tyrosine, L-tyramine, L-DOPA, L-dopamine was purchased from Aladdin Co., Ltd. (Shanghai), pyridoxal 5'-phosphate (PLP) was purchased from Sigma-Aldrich Co., Ltd. (St. Louis, MO, USA), Sodium acetate trihydrate, Trifluoroacetic acid were purchased from , KOD-Plus-Neo DNA polymerase and *Dpn*I was purchased from Toyobo Co., Ltd. (Osaka, Janpan).

1.2 Site-directed Mutagenesis

Site-directed mutagenesis performed by whole plasmid PCR and use recombinant *pet*24a-*Lb*TyDC coding as a template. The PCR amplification system contained complementary primers and uses KOD-Plus-Neo DNA polymerase to amplification sequence. PCR program was: pre-denaturation at 94°C for 4 min, followed by amplification for 25 cycles with denaturation at 98°C for 10 s, annealing at 55°C for 15 s and elongation at 72°C for 5 min, and then further elongation at 72°C for 10 min. The plasmids verified by nucleic acid glue and digested with 1 μL of *Dpn*I for 0.5 h at 37°C to remove the methylated templates. Then 10 μL of the digestion mixture were transformed into *E. coli* BL21 (DE3). Single colonies were picked up and cultivated on LB medium (50 μg/mL Kan). The plasmids of mutations were confirmed by sequencing.

1.3 Protein expression and purification

Recombinant *E. coli* BL21 (DE3) including ^{WT}*Lb*TyDC and variants were cultivated at 37°C and 180 rpm in LB medium supplemented with 1% glucose. Until OD_{600} reached 0.6~0.8, induced with 0.2mM isopropyl β-D-thiogalactopyranoside(IPTG)

and further cultivated at 25°C. and 180 rpm for 6 h. The induced cell were harvested by centrifugation (4°C, 8,000×g for 10 min) and the cell resuspended with phosphate buffer A (25 mM Tris-HCl, 300 mM NaCl, 20 mM imidazole, 5 mM β-mercaptoethanol, pH 7.4), then disrupted with ultra-sonication (work for 2 s, pause for 3 s, 150 W). The resulting supernatant was loaded onto a His-Trap HP nickel affinity column pre-equilibrated with buffer A using AKTA Avant System (GE Healthcare, USA), TyDC was eluted off by a 20-300 mM imidazole gradient in buffer B(25 mM Tris-HCl, 300 mM NaCl, 300 mM imidazole, 5 mM β-mercaptoethanol,pH 7.4). The collected proteins were verified by SDS-PAGE analysis and then concentrated by an ultrafiltration tube. The target pure enzyme is subjected to the next experiment.

1.4 Enzymatic activity and kinetic assay

Typical reaction assay mixtures of 1 mL containing 10 μL TyDC enzyme that diluted to an appropriate amount，2 mM L-tyrosine or L-DOPA in sodium acetate buffer (0.2 M, pH 5.0) and 0.2 mM PLP, incubated at 40°C in a water bath. The reaction were stopped at 10 min by boiling at 100°C for 10 min. After centrifugated at 12000×g for 5 min, taking the supernatant for HPLC detection. L-tyrosine, L-tyramine, L-DOPA, and L-dopamine levels were determined by high-performance liquid chromatography (HPLC) (Agilent 1260, USA) using Diamonsil C18 column (DIKMA, China) with water/methanol (90:10, v/v) as mobile phase at 220 nm and 30°C with a flow rate of 1 $mL \cdot min^{-1}$. One unit of activity was defined as the amount of enzyme that was required for the production of 1.0 μmol L-tyramine or L-dopamine per minute under the enzymatic activity addition.The kinetic assay was detected employing the standard activity assay method, in the presence of different concentrations of L-tyrosine and L-DOPA from 0.1 to 5.5 mM. Substrate reduction or product increase were determined

by HPLC. All the activities were determined in triplicate and averaged to obtain the kinetic parameters. The K_m, V_{max} and k_{cat} were calculated according to the Lineweaver-Burk plot.

1.5 Isothermal titration calorimetry

The binding affinity and binding enthalpy between *Lb*TyDC and PLP was measured using a PEAQ-ITC (MICROCAL PEAQ-ITC) at 30°C. The enzyme was purified as the method above. Protein sample at 100 μM was prepared in sodium acetate buffer (0.2 M, pH 5.0), PLP sample at 1 mM was dissolved in the same buffer. For titrations of *Lb*TyDC with PLP, 2 μL of 1 mM PLP was injected 19 times and each injection was monitored at 150-second intervals. Titrating the same PLP sample to sodium acetate buffer (0.2 M, pH 5.0) with the same procedure everytime as a control. The collected data was processed by MicroCal PEAQ-ITC Analysis Software.

1.6 Molecular dynamics simulations

The initial protein structure used in the PRS analysis was constructed with holo protein structure,[1] in which the missing segments A418-G425 of Chain A and N45-S49 and F417-L431 of chain B were made up with the "model/refine loop" module in software Chimera (UCSF Chimera, version 1.13.1, 2018).[2] The turn-over-determining transition state (TDTS) has been computed in the previous literatures, as the de-carboxylate step between external aldimine and quinonoide intermediate[3]. Thus the external-aldimine complexation of substrate and the enzyme was constructed after breaking down internal aldimine of Lys392. The enzyme-substrate complexes were further optimized with the CHARM force field in Discovery Studio software package 3.5. The external-aldimine substrate was structurally optimized with the semi-empirical method (AM1) and parameterized for the following-up molecular dynamic simulation with the antechamber program in the Gaussian16 (Gaussian 16, Revision

B.01)[4] and AMBER12 software package[5]. Water molecules was assigned with the TIP3P model, and the general Amber force field (GAFF) and ff03.r1 force field were applied for the classical molecular dynamics simulation. The complexes were placed in a truncated octahedral box of water molecules, extending 10.0 Å along each dimension. A certain number of counterions Na+ were added to neutralized the calculated system. The MD systems were first minimized by the steepest descent minimization of 1000 steps followed the conjugate gradient minimization of 9000 steps, heated up from 0 to 300 K at constant volume in 50 ps, and equilibrated for another 50 ps without any restraints. In the MD simulations, the Particle Mesh Ewald (PME) method was employed for long-range electrostatic interactions. Finally, multiple 10 ns of trajectories with partially breaking C--C bond (about 2.2Å in transition structure) were collected for the further PRS analysis, similar to our previous studies.[6-10]

1.7 Quantum mechanical calculations

The decarboxylation of external aldimine was calculated with the theozyme model at the wB97x-D(CPCM, water)/6-31G(d) method, using the starting structure extracted from the protein-enzyme complex in the above molecular dynamics simulation. The NBO population analysis was conducted on each point along the intrinsic reaction coordinate, with Gaussian 09 software.

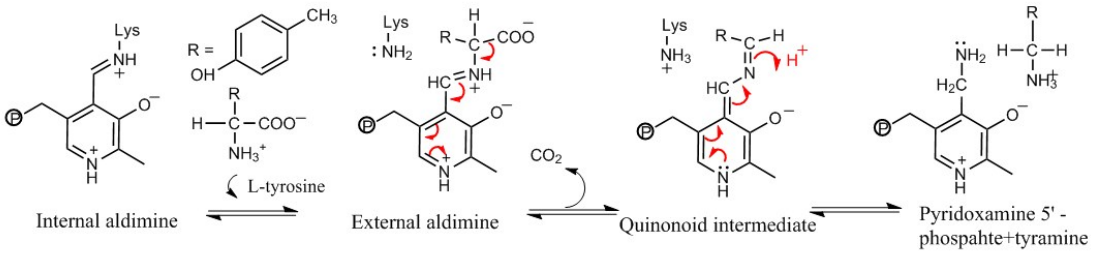

Figure S1. Currently accepted mechanism for the reaction catalyzed by TyDC.

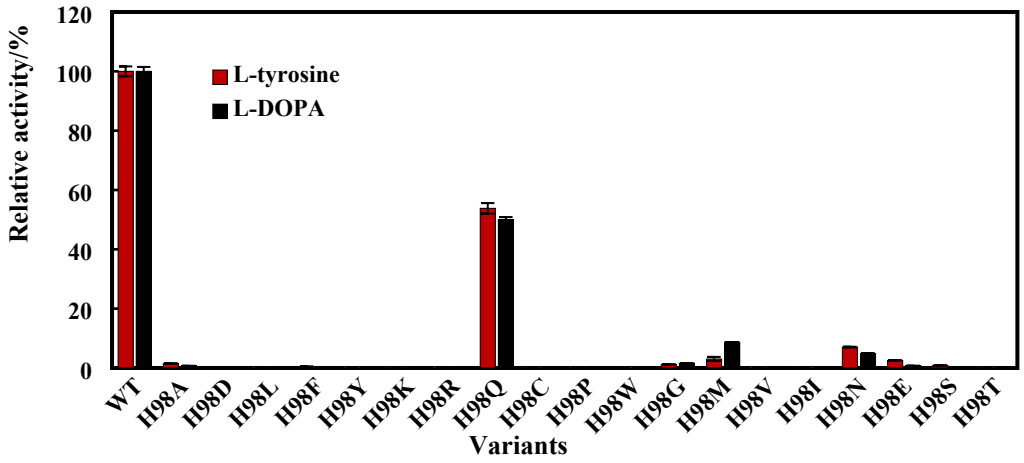

Figure S2. Relative activities of ^{WT}*Lb*TyDC and variants of His98 towards L-tyrosine and L-DOPA. The activities of ^{WT}*Lb*TyDC enzyme toward L-tyrosine and L-DOPA are set to 100%. Red bar: L-Tyrosine, black bar: L-DOPA.

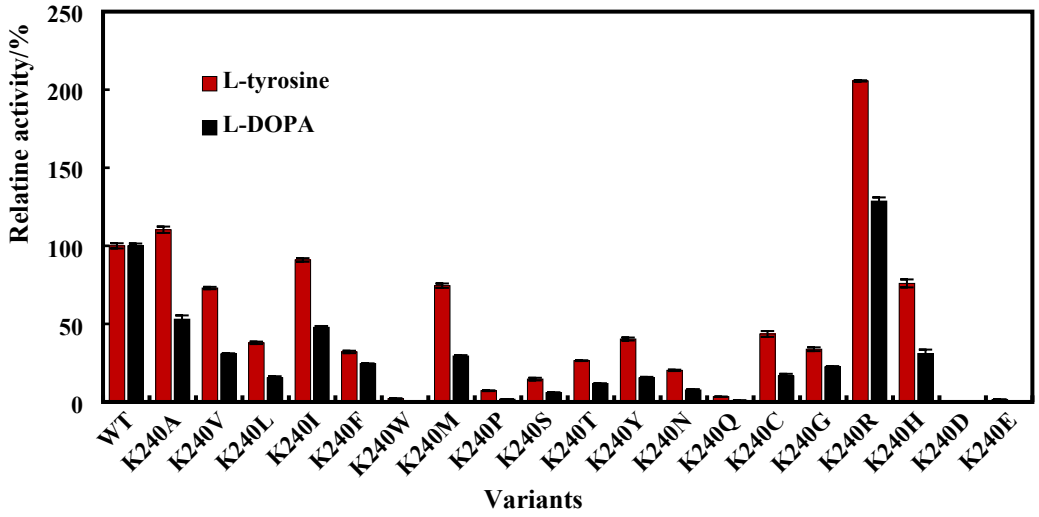

Figure S3: Relative activities of ^{WT}*Lb*TyDC and variants of Lys240 towards L-tyrosine and L-DOPA. The activities of ^{WT}*Lb*TyDC enzyme toward L-tyrosine and L-DOPA are set to 100%. Red bar: L-Tyrosine, black bar: L-DOPA.

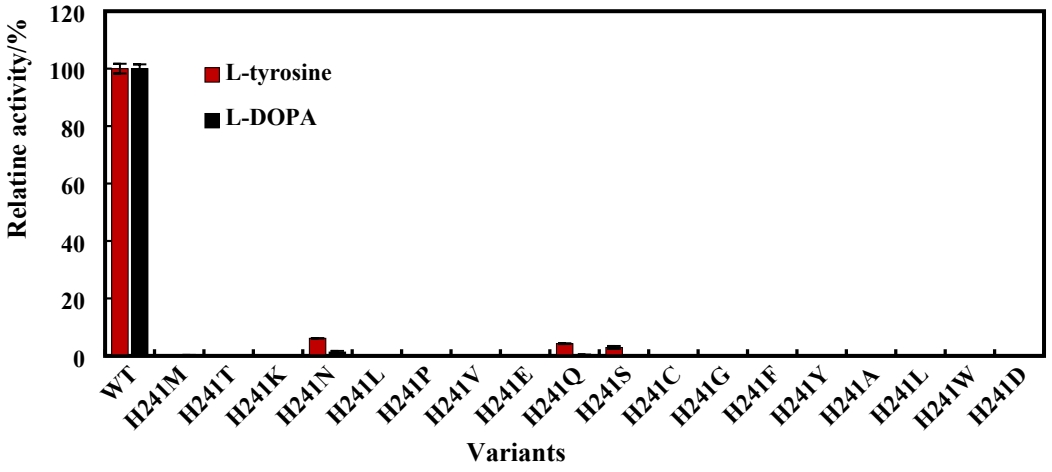

Figure S4. Relative activities of ^{WT}*Lb*TyDC and variants of His241 towards L-tyrosine and L-DOPA. The activities of ^{WT}*Lb*TyDC enzyme toward L-tyrosine and L-DOPA are set to 100%. Red bar: L-tyrosine, black bar: L-DOPA.

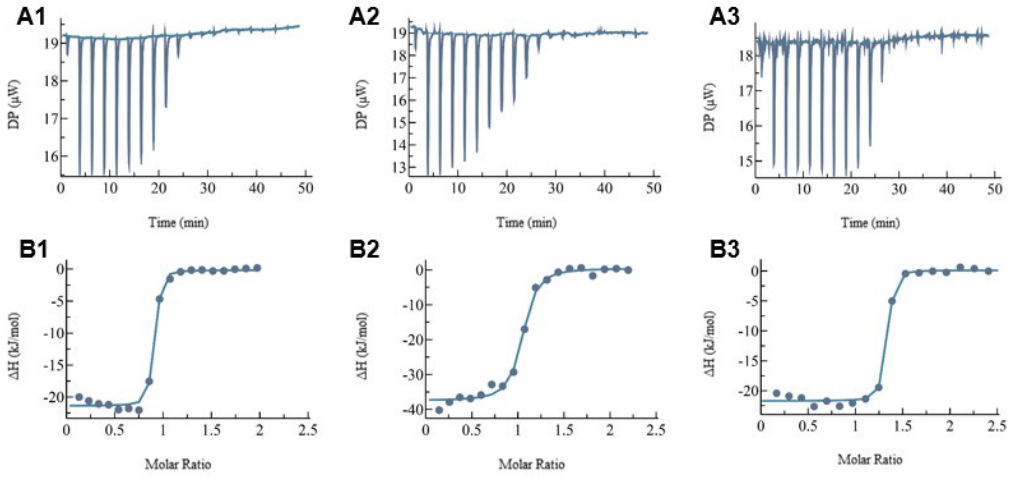

Figure S5. Raw (A1, A2, A3) and fitted (B1, B2, B3) data of Isothermal titration calorimetry of ^{WT}*Lb*TyDC and mutants. ^{WT}*Lb*TyDC (A1 and B1); H241A (A2 and B2); H241F (A3 and B3). The binding interactions between ^{WT}*Lb*TyDC and PLP were carried out using a PEAQ-ITC (MICROCAL PEAQ-ITC). The collected data was processed by MicroCal PEAQ-ITC Analysis Software.

Table S1. Binding affinity and binding enthalpy between ^{WT}*Lb*TyDC/mutants and PLP.

Enzyme	K_D (10^{-2} μM)	ΔH（kcal/mol）
WT	7.32±0.2	-5.07±0.1
H241A	48.1±1.2	-9.06±0.2
H241F	3.81±0.1	-5.21±0.7

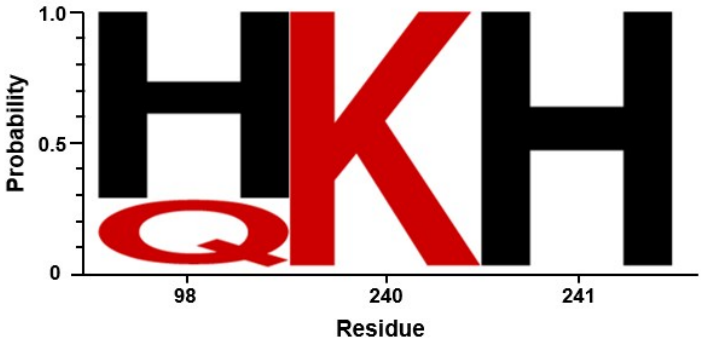

Figure S6 Consensus analysis of His98, Lys240 and His241. Sequences of tyrosine decarboxylase with more than 40% identities were selected for analysis. All protein sequences used were obtained from the National Center for Biotechnology Information (https://www.ncbi.nlm.nih.gov/). Multiple sequence alignments were performed using the software of BioEdit and WebLogo (http://weblogo.berkeley.edu/logo.cgi).

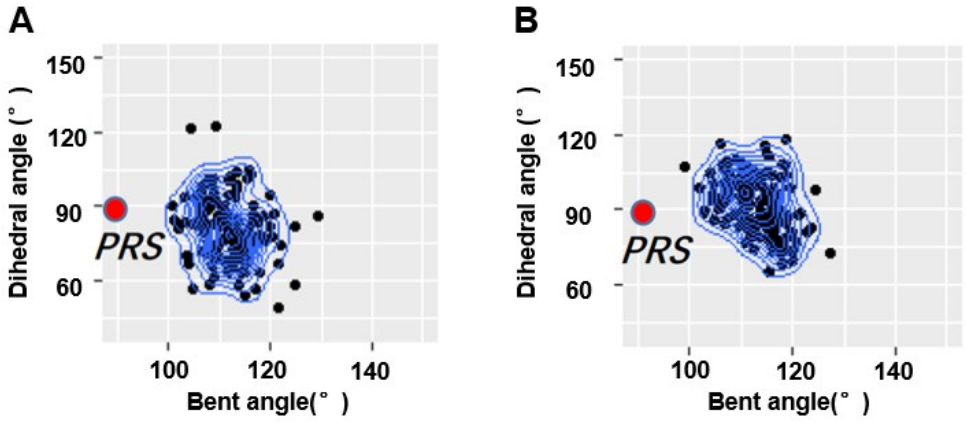

Figure S7. Probability density distribution of C-Cα-N_{SB}-C4′ dihedral angles in H98M with L-tyrosine and L-DOPA as the substrate. (A) H98M with L-tyrosine sampled during MD simulation. PRS-best orbital overlapped conformation. (B) H98M with L-DOPA sampled during MD simulation.

Table S2. Cartesian coordinates (in Å) of external aldimine for quantum mechanical calculations.

O	4.9550	0.3008	-3.2095
H	4.7514	1.1969	-3.5081
C	4.2195	0.0243	-2.0943
C	3.3334	0.9397	-1.5305
C	2.6191	0.6033	-0.3832
H	1.9460	1.3393	0.0508
H	3.1982	1.9220	-1.9778
C	4.3826	-1.2327	-1.5070
H	5.0784	-1.9393	-1.9493
C	3.6639	-1.5549	-0.3617
H	3.8083	-2.5330	0.0932
C	2.7747	-0.6447	0.2203
C	2.0074	-0.9840	1.4770
H	2.6885	-1.3698	2.2446
H	1.5390	-0.0763	1.8731
C	0.9416	-2.0736	1.2931
C	0.3028	-2.3985	2.7035
O	0.9219	-3.2666	3.3533
O	-0.6948	-1.7208	3.0225
H	1.4043	-2.9830	0.9043
N	-0.1081	-1.7202	0.3555
H	-0.5372	-2.4697	-0.2093
C	-0.7839	-0.6122	0.3547
H	-0.4014	0.2426	0.9278
C	-2.0157	-0.5078	-0.4002
C	-2.5160	-1.6557	-1.1092
O	-1.9286	-2.7690	-1.1978
C	-3.8069	-1.5015	-1.7495
C	-4.4254	-2.6448	-2.4735
H	-4.5463	-3.4881	-1.7866
H	-3.7585	-2.9791	-3.2738
H	-5.3974	-2.3868	-2.8993
N	-4.4290	-0.3345	-1.6744
H	-5.3292	-0.2490	-2.1382
C	-3.9599	0.7645	-1.0220
H	-4.5873	1.6436	-1.0563
C	-2.7564	0.6996	-0.3697
C	-2.2679	1.9245	0.3699
H	-3.0566	2.6905	0.3483
H	-2.1086	1.6571	1.4238
O	-1.0870	2.3893	-0.2173
P	0.0333	3.0887	0.8853
O	1.1401	3.5328	-0.0630
O	0.3926	1.9071	1.8023
O	-0.7421	4.2039	1.5769

Reference:

1 H. Zhu, G. Xu, K. Zhang, X. Kong, R. Han, J. Zhou and Ni. Y, *Sci. Rep*., 2016, **6**, 27779.

2 A. Waterhouse, M. Bertoni, S. Bienert, G. Studer, G. Tauriello, R. Gumienny, F. T. Heer, T.A.P de Beer, C. Rempfer, L. Bordoli, R. Lepore and T. Schwede, *Nucleic Acids Res*, 2018, **46**, W296-W303.

3 H. S. Fernande, M. J. Ramos and N. Cerqueira, *Chem.-Eur. J.*, 2017, **23**, 9162-9173.

4, M. J. Frisch, G. W. Trucks, H. B. Schlegel, G. E. Scuseria, M. A. Robb, J. R. Cheeseman, G. Scalmani, V. Barone, G. A. Petersson, H. Nakatsuji, X. Li, M. Caricato, A. V. Marenich, J. Bloino, B. G. Janesko, R. Gomperts, B. Mennucci, H. P. Hratchian, J. V. Ortiz, A. F. Izmaylov, J. L. Sonnenberg, D. Williams-Young, F. Ding, F. Lipparini, F. Egidi, J. Goings, B. Peng, A. Petrone, T. Henderson, D. Ranasinghe, V. G. Zakrzewski, J. Gao, N. Rega, G. Zheng, W. Liang, M. Hada, M. Ehara, K. Toyota, R. Fukuda, J. Hasegawa, M. Ishida, T. Nakajima, Y. Honda, O. Kitao, H. Nakai, T. Vreven, K. Throssell, J. A. Montgomery, Jr., J. E. Peralta, F. Ogliaro, M. J. Bearpark, J. J. Heyd, E. N. Brothers, K. N. Kudin, V. N. Staroverov, T. A. Keith, R. Kobayashi, J. Normand, K. Raghavachari, A. P. Rendell, J. C. Burant, S. S. Iyengar, J. Tomasi, M. Cossi, J. M. Millam, M. Klene, C. Adamo, R. Cammi, J. W. Ochterski, R. L. Martin, K. Morokuma, O. Farkas, J. B. Foresman, and D. J. Fox, *Inc., Wallingford CT*. 2016.

5 D. A. Case, T. A. Darden, T. E. Cheatham, C. L. Simmerling, J. Wang, R. E. Duke, R. Luo, R. C. Walker, W. Zhang, K. M. Merz, B. Roberts, S. Hayik, A. Roitberg, G. Seabra, J. Swails, A. W. Götz, I. Kolossvary, K. F. Wong, F. Paesani, J. Vanicek, R.

M. Wolf, J. Liu, X. Wu, S. R. Brozell, T. Steinbrecher, H. Gohlke, Q. Cai, X. Ye, J. Wang, M. J. Hsieh, G. Cui, D. R. Roe, D. H. Mathews, M. G. Seetin, R. Salomon-Ferrer, C. Sagui, V. Babin, T. Luchko, S. Gusarov, A. Kovalenko and P. A Kollman, 2012.

6 B. He, T. Zhou, X. Bu, J Weng, J. Xu, S. Lin, J. Zheng, Y. Zhao and M. Xu, *ACS Catal*., 2019, **9**, 5391−5399.

7 Z. Zhang, C. S. Jamieson, Y. Zhao, D Li, M. Ohashi, K. N. Houk and Y. Tang, 2019, *J. Am. Chem.Soc.*, 2019, **141**, 5659–5663.

8 J. Zhou, Y. Wang, G. Xu, L. Wu, R. Han, U. Schwaneberg, Y. Rao, Y. Zhao, J. Zhou and Y. Ni, *J. Am. Chem.Soc.*, 2018, **140**, 12645-12654.

9 T. Shi, L. Liu, W. Tao, S. Luo, S. Fan, X. Wang, L. Bai and Y. Zhao, *ACS Catal.*, 2018, **8**, 4323-4332.

10 X. Chen, T. Shi, X. Wang, J. Wang, Q. Chen, L. Bai and Y. Zhao, *ACS Catal.*, 2016, **6**, 4369-4378.